ELSEVIER

Journal of Hydrology 243 (2001) 31–42

Journal of Hydrology

www.elsevier.com/locate/jhydrol

Investigating short-term dynamics and long-term trends of SO_4 in the runoff of a forested catchment using artificial neural networks

G. Lischeid*

Hydrogeology Department, BITÖK, University of Bayreuth, Dr. Hans-Frisch-Str. 1-3, 95440 Bayreuth, Germany

Received 7 July 2000; revised 9 October 2000; accepted 1 November 2000

Abstract

The impact of long-lasting non-point emissions on groundwater and streamwater in remote watersheds has been studied at numerous sites. In spite of substantially decreasing emissions in the last decade, recovery has not yet been observed in all cases. This trend might be masked by the considerable short-term variability of the chemical hydrographs. In this study, artificial neural networks are applied to investigate the SO_4 dynamics in the runoff of a small forested catchment susceptible to SO_4 deposition. Empirical models are fitted to the short-term dynamics at a time step of one day. About 75% of the variance of the SO_4 data is explained by the instantaneous discharge, short-term history of discharge and the moving average of SO_4 concentration in throughfall. In contrast, neither air temperature as an indicator for biological activity nor a snowmelt indicator based on the temperature sum increase the performance of the model. The model is used to investigate long-term trends in sub-regions of the phase space spanned by the identified input variables. According to the model, decreasing emissions have a significant effect on runoff SO_4 concentration only during the first severe storms at the end of the vegetation period. This suggests to focus on these events as indicators for recovery of the topsoil layers. © 2001 Elsevier Science B.V. All rights reserved.

Keywords: Artificial neural network; Discharge; Sulfate; Freshwater; Trend analysis

1. Introduction

Small catchments have been studied intensively in order to assess their future development under human influence. Now numerous long-term hydrochemical data series are available. Here, time series of sulfate concentration in the runoff of a small-forested catchment are studied. Although sulfate emissions decreased substantially in the last two decades (Stoddard et al., 1999), there is no clear trend of sulfate concentration in the catchment's runoff. The pronounced short-term dynamics of the data set are likely to represent a variety of interrelated processes at different scales that might mask long-term trends.

Often deterministic, physically based models are used for analyzing data sets of that kind. To avoid over-parameterization (Beven, 1993), only a very limited set of processes selected in an ad hoc manner can be considered. However, it has been stated that independent falsification or validation of a model, and thus unequivocal process identification by modeling is not possible (Oreskes et al., 1994). Furthermore, there seems to be a lack of consistency in approach (Hauhs et al., 1996). Facing the apparent complexity of environmental systems, the physical basis of the equations used within lumped models needs to be challenged and has been shown to be deficient (Neal, 1997). Obviously, the substantial heterogeneity encountered within natural systems has to be taken into account, e.g. by complexity theory based approaches or fractal

* Tel.: +49-921-555632; fax: +49-921-555799.

0022-1694/01/$ - see front matter © 2001 Elsevier Science B.V. All rights reserved.
PII: S0022-1694(00)00399-1

Table 1
Mean budget for the Lehstenbach catchment November 1987–October 1996. Units are mm a^{-1} and kmol ha^{-1} a^{-1}, respectively. The data were kindly provided by K. Moritz and J. Bittersohl of the Bavarian State Office for Water Management

	H_2O	H^+	Cl	SO_4	NO_3	Ca	Mg	Na	K	NH_4	Al
Bulk precip.	951	0.39	0.18	0.33	0.49	0.16	0.03	0.30	0.07	0.57	0.00
Throughfall	768	1.64	0.33	1.31	0.77	0.39	0.10	0.33	0.61	0.71	0.00
Runoff	450	1.18	0.91	1.00	0.38	0.47	0.19	1.13	0.12	0.02	0.23

analyses (cf. Kirchner et al., 2000). In addition, it has been suggested to return to purely empirical models that are adequate for the information content in field data (Peters, 1991). Revealing the internal structure of the given data set by empirical models helps to identify processes in a top–down approach as part of an iterative process (Christophersen and Neal, 1990).

Here an artificial neural network is applied. It allows for analyzing multiple non-linear relationships and for performing sensitivity analyses for individual parameters. Long-term trends can be investigated by analyzing shifts in the regression planes revealed by the model.

2. Data set

A long-term monitoring program started in 1987 in the 4.2 km^2 Lehstenbach catchment in the Fichtelgebirge mountains in Southern Germany (North East Bavaria) (Sager et al., 1990; Lischeid et al., 1998a). The thickness of the regolith overlying the granite bedrock is about 30–40 m. Among the soils, dystric cambisols predominate. One third of the catchment is covered by peaty soils and bogs. The catchment is drained by a dense and irregular network of brooks and ditches.

The altitude of the catchment is 690–877 m asl. Long-term mean annual precipitation sums to 1100 mm, but has been considerably less in the years of the study (Table 1). Annual mean temperature at the mountain top is 4.5–5°C. The catchment is nearly completely covered by a spruce forest (*Picea abies* (L.) Karst.).

Discharge at the catchment outlet is measured continuously. Samples are taken biweekly at least. The total number of analyses available is 384 covering the November 1987–March 1998 period.

Throughfall has been investigated biweekly at up to seven different plots in the catchment with 15 replicates each. Additionally, bulk precipitation has been measured at three different plots. Groundwater has been sampled every 4–8 weeks at six wells in the catchment since 1987, and at additional eight wells since 1996 by a submersed pump.

Mean budgets for the catchment are given in Table 1. SO_4 input via throughfall is more than fourfold SO_4 bulk precipitation input due to occult deposition. On the other hand, SO_4 output is about 3/4 of SO_4 input via throughfall. Nitrogen output is 2/5 of N input via bulk precipitation. Cl and Na output in runoff exceeds the input because of salting of a public road in the western part of the catchment. Increasing the ionic strength by road salt application seems to have only minor effects on SO_4 dynamics, as time series of SO_4 concentration of the western and the eastern main tributary differ only slightly.

3. Artificial neural networks

Artificial neural networks (ANN) are now increasingly used in a wide variety of problems, dealing with pattern recognition in a broad sense. Examples of applications of ANN in hydrological studies are given by Maier and Dandy (1996), Clair and Ehrman (1998), Shamseldin (1998), and Luk et al. (2000). They make use of the capability of ANN to map multivariate, non-linear relationships to an arbitrary accuracy (Hornik et al., 1989).

3.1. Structure

In this study, a multilayer feedforward network is used. It is composed of a number of nodes, which are arranged in consecutive layers: an input layer, a number of hidden layers, and an output layer. The number of nodes in the input layer corresponds to the number of input variables, and the number of

nodes in the output layer to that of the output variables, respectively. The number of hidden layers, and the number of nodes in these layers can be chosen arbitrarily. Usually, the network topology is given by a $x_i{:}x_h{:}x_o$ notation, where x_i, x_h, and x_o denote the number of nodes in the input, hidden, and output layer, respectively. Every node is connected with every node of the subsequent layer by weighted connections. Data processing is unidirectional from the input layer towards the output layer ('feedforward').

For all nodes, an input function, an activity function and an output function is defined. In this case, the functions are the same for all nodes. Usually, the input function net_j is given by:

$$\mathrm{net}_j = \sum_{i=1}^{n} w_{ij} o_i$$

where i and j are the indices for the nodes in the preceding and actual layer, respectively, n the number of nodes in the preceding layer, w_{ij} the weight of the connection between single nodes, and o_i the output value of node i.

The activity function o_j has to be a monotonous, differentiable function. Here, usually the Fermi function is used:

$$o_j = \frac{1}{1 + \mathrm{e}^{-\mathrm{net}_j}} - \theta_j$$

Introducing a bias θ_j allows for a constant offset of the weighting function, thus shifting the most sensitive part of the weighting function (that is, the part of the steepest increase).

The software used in this study is the Stuttgart Neural Network Simulator (SNNS), version 4.1, developed by Zell et al. (1995). It is a tool for editing, training, testing and visualization of neural networks, written in ANSI-C. A variety of different network types, learning algorithms, pruning algorithms, error measures, and tools for analyzing the networks is offered. A graphical user interface allows for convenient editing of networks. Training and testing of networks can be performed on-line as well as in a batch mode.

3.2. Training

Weights and biases are optimized in a procedure called 'learning' or 'training'. For every input pattern the output (o_j) is compared with the output given (t_j = 'teaching output') and the weight matrix is corrected iteratively.

The training of the network aims to minimize the sum of squared errors. As a measure of comparing the performance of different simulation runs the model efficiency r_{eff} (Nash and Sutcliffe, 1970) is used. It is defined as

$$r_{\mathrm{eff}} = 1 - \frac{\sigma^2_{xx'}}{\sigma^2_{xx}}$$

where $\sigma^2_{xx'}$ is the mean squared error of the simulation, and σ^2_{xx} the sum of squared differences between measured values and their mean. If the relationship between measured and simulated data happens to be linear, r_{eff} can be interpreted as the explained part of the total variance of the data set.

A variety of different methods exist to solve the principal problems of the training procedure. First, the aim is to map the essentials of the total ensemble ('generalization') rather then specific features of the random sample available for the training of the network ('overtraining'). Second, there is only a trial-and-error approach to distinguish between a local and the global minimum of the error plain. Third, different training algorithms differ substantially with respect to the convergence velocity.

In a first phase, different learning functions were tested (Quickprop, Resilient Propagation and Backpercolation; see Zell et al., 1995 for details). In this study, the Resilient Propagation (Rprop) method yielded superior performance and was used for the subsequent training runs. Like the well-known Backpropagation algorithm (Rumelhart and McClelland, 1986), it is a gradient descent method. In contrast to the latter, the basic idea is to decrease the update value of the weight w_{ij} when the partial derivative of the error function changes its sign, and to increase it otherwise (Riedmiller and Braun, 1993).

Following the usual cross validation approach, the total data set is subdivided into a training, validation and test data set. Every 1000 training cycles the network error (sum of squared errors) is determined both for the training and the validation data set. If the network error is not inferior to that of the preceding test, the weight matrix is altered by random factors in

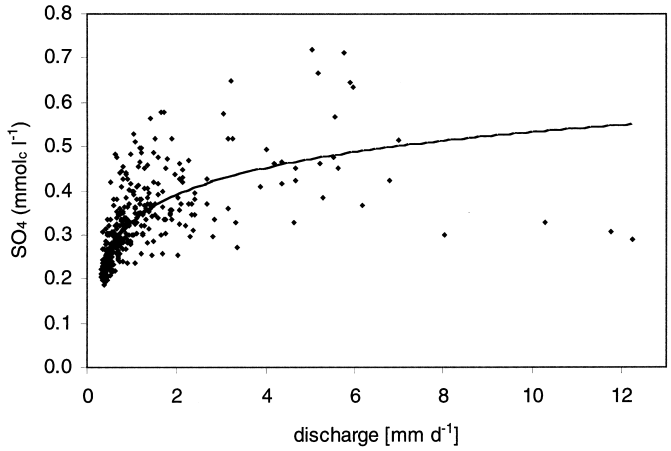

Fig. 1. Measured (diamonds) and fitted (solid line) SO_4 concentration versus daily mean discharge at the catchment's outlet.

the [0;2] range. Otherwise, the weight matrix is saved and training continues. Performance of the network applied to the test data set after the training should not be substantially less than for the validation data set.

The total number of training cycles per training run was 5×10^5. In most cases, however, model efficiency of the network increased by less than 0.02 after the first 10^5 training runs. Effects of different random initializations of weights and biases were accounted for by 10 replicates of every training run.

3.3. Preprocessing the data set

How to divide the total data set into the three subsets is extensively discussed in the literature (Baum and Haussler, 1989; Maier and Dandy, 1996). In practice, the limited size of most data sets suggests that the major part be taken for the training data set. The data were therefore split up randomly in a 2:1:1 ratio for the training, validation and test data set, respectively. This procedure is repeated ten times each for every model.

Input variables are selected partly based on expert's knowledge, partly on availability. A preceding bivariate fitting revealed that instantaneous discharge explains most of the variance of the SO_4 time series in the catchment's runoff. Fitting a logarithmic function to the data yields a model efficiency of about 0.49. However, the large scatter of this relationship (Fig. 1) is a challenge for a more sophisticated approach.

In addition to mean discharge, air temperature is chosen. To account for the short-term memory of the system that is not accounted for explicitly by the type of neural network used, in addition to the temperature of the day of streamwater sampling (d), mean temperature values of preceding days (d − 1), (d − 2), (d − 3), (d − 5), (d − 10) and (d − 30) are chosen as well as the mean of the preceding 5 (m 5d) and 30 (m 30d) days period, respectively (cf. Luk et al., 2000).

To investigate the impact of snowmelt on SO_4 dynamics, summed daily mean temperature values since last exceedance of 0°C are used as a snowmelt indicator. Snow cover data that are available for the 1996–1998 period confirm that low positive values are indeed closely related to snowmelt.

The first visual inspection of the data revealed that SO_4 concentration of the catchment's runoff during the first discharge peaks after the end of the vegetation period seemed to be higher than during subsequent stormflow events. Thus another indicator is introduced to provide the network with necessary information, called 'accumulated runoff'. Even during extended baseflow periods, discharge was never less than 0.2 mm day^{-1}. On the other hand, discharge peaks usually substantially exceed 0.5 mm day^{-1}. Thus 0.5 mm day^{-1} is chosen as a threshold value to distinguish baseflow from stormflow conditions.

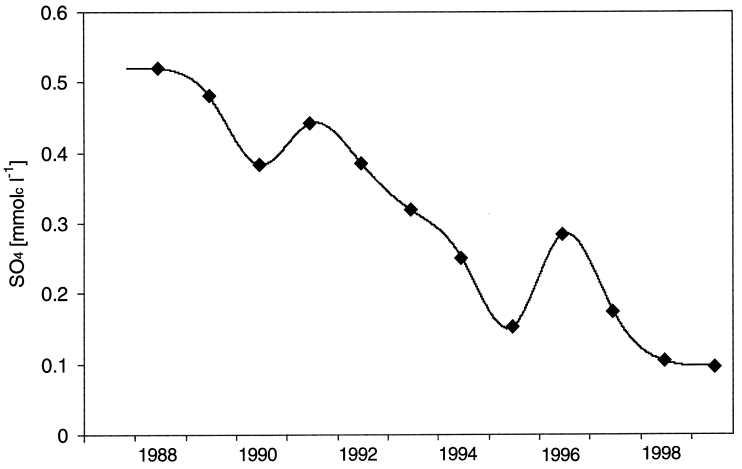

Fig. 2. SO_4 concentration in the Lehstenbach catchment's throughfall. Shown are measured mean values for single years and interpolated data for the model input, respectively.

Daily mean runoff is then accumulated as long as it exceeds the threshold value, and is set equal to the daily mean discharge otherwise.

Sulfate concentration in the throughfall was measured by bulk samples in biweekly intervals. However, the number and location of single sites has been subject to numerous changes. In addition, sampling dates have not always been the same for all sites. On the other hand, the model requires daily input data. To represent the long-term trend of throughfall concentration within the model, the yearly mean concentration data were interpolated by a cubic spline (Fig. 2).

3.4. Minimizing the network

To reduce the danger of overfitting, both the numbers of input and of hidden nodes should be minimized. This was done by a pruning approach. First, 100 networks are trained with all of the 21 input variables described above. The single networks differ only with respect to subdivision of the total data set and initialization of the weight matrix. In a second step, pruning of input and hidden nodes is performed subsequently by skeletonization (Mozer and Smolensky, 1989). Parameters of the skeletonization algorithm are the same

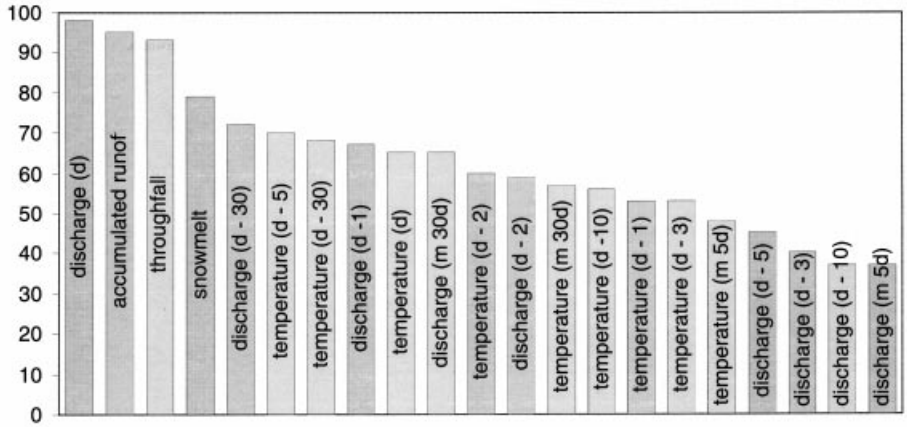

Fig. 3. Number of cases (out of 100) where single variables are selected as relevant by the skeletonization procedure.

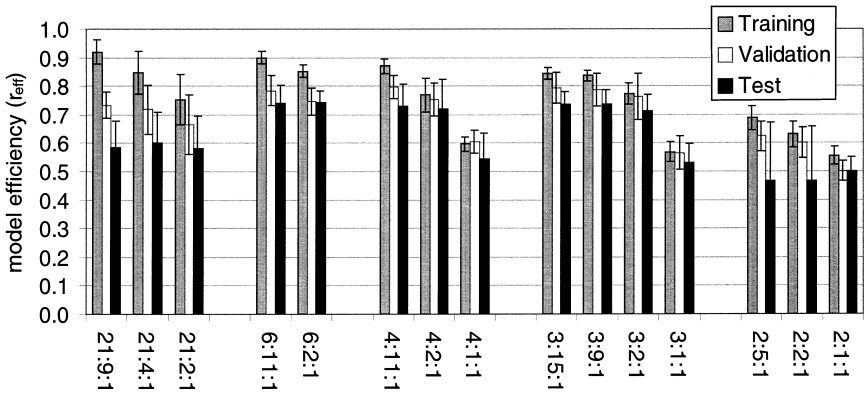

Fig. 4. Model efficiency for different networks for the training, validation and test data set, respectively. Mean and standard deviation for 100 networks each are shown. The label at the *x*-axis indicates the network topology ($x_i : x_h : x_o$), with x_i, number of input nodes, x_h, number of nodes in the hidden layer, and x_o, number of nodes in the output layer. Input variables are the first *n* variables given in Fig. 3.

for all of the 100 networks. The results are used as a ranking of relevance of input nodes.

In a second step, networks are trained using only the most relevant input variables with different numbers of hidden nodes. Again, 100 replicates are used for every network topology. The criterion for selection of the best among these networks is minimum standard deviation of network efficiency within and between the training, validation and test data sets with 100 replicates each.

4. Results

4.1. Minimizing the network

Results of the skeletonization procedure are given in Fig. 3. In more than 90 out of 100 networks, instantaneous discharge, accumulated runoff and throughfall concentration are selected as relevant driving variables by the skeletonization procedure. The snowmelt indicator variable is selected in 79 cases, air temperature and discharge of preceding days in 70 cases or less.

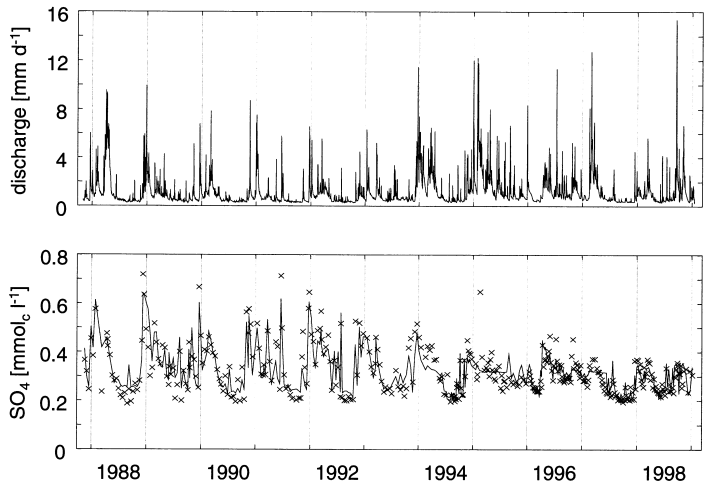

Fig. 5. Time series of discharge (upper panel) and measured (solid line) and simulated (×) SO_4 concentration (lower panel) of the catchment's runoff.

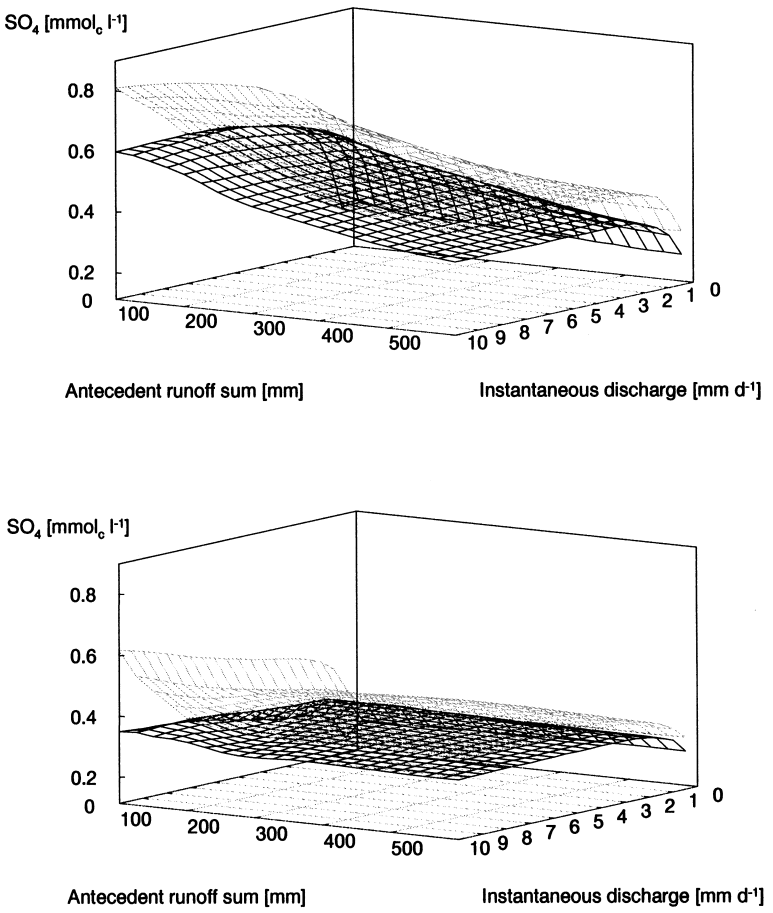

Fig. 6. SO_4 concentration in the catchment's runoff depending on instantaneous discharge and antecedent runoff sum predicted by the model. Mean SO_4 concentration in the throughfall is 0.5 $mmol_c\,l^{-1}$, corresponding to mean concentration measured in 1988 (upper panel) and 0.1 $mmol_c\,l^{-1}$, corresponding to mean concentration measured in 1998 (lower panel), respectively. See Fig. 2 for time series of SO_4 deposition. Grey plane, mean + standard deviation; black plane, mean − standard deviation ($n = 100$) for every grid point.

Performance of different networks is given in Fig. 4. As expected, the network with 21 input variables yields the highest model efficiency for the training data set, but substantially lower efficiency for the validation and test data set. This is clear evidence for overtraining of the network. Decreasing the number of hidden nodes down to two does not have a significant impact on the model performance.

Subsequently reducing the number of input variables according to the skeletonization ranking reduces the model efficiency for the training data set, but tends to increase it for the validation and test data set. The number of input variables can be reduced down to three (instantaneous discharge, accumulated runoff and throughfall concentration) without any loss of network performance for the validation and the test data sets. The model efficiency for the 3:2:1 network is about 0.75. Again, introducing more than two hidden nodes does not improve the network significantly. Omitting throughfall concentration as driving variable, however, substantially deteriorates the model. Here, increasing the number of hidden nodes tends to improve the model with respect to the training and validation data set, but only at the cost of substantially increasing the standard deviation of model

efficiency for the test data set. This is a clear evidence for a decreasing generalization capability.

Fig. 5 presents time series of measured and simulated SO_4 concentration in the runoff. Among the 100 3:2:1 networks that with the least variance of model efficiency between the three subsets is selected. Model efficiency is 0.77, 0.75 and 0.74 for the training, validation and test data set, respectively. In most cases, the model nicely depicts the concentration peaks. There is some evidence that the high SO_4 concentration measured in the beginning of 1995 is an artifact.

4.2. Visualization of dependencies revealed by the model

Besides identifying driving variables, the visualization of the multivariate interdependencies is a further step to studying the predominating dependencies. Based on the criteria given above, the 3:2:1 model has been selected as the 'best' model. Fig. 6 shows the dependencies between the driving variables and SO_4 concentration in the catchment's runoff, as revealed by the model. The two planes indicate mean $\pm$ standard deviation of 100 networks for every input tuple of input variables. In principle, SO_4 concentration increases with instantaneous discharge but tends to level off for discharge >3 mm day^{-1}.

Obviously the most pronounced effect of decreasing SO_4 concentration in throughfall is restricted to high values of instantaneous discharge and low values of accumulated runoff. This characterizes the first storms at the end of the vegetation period. For these storms, SO_4 concentration decreased by a half due to decreasing throughfall concentration. Correspondingly, the prognostic value of the accumulated runoff diminishes with decreasing throughfall concentration.

5. Discussion

5.1. Minimizing the network

The artificial neural network provides a tool to estimate the minimum model complexity needed to map certain patterns. In general, the simpler the model, the more reliable and the easier to interpret are the results.

Often the complexity of a successfully trained network is reduced by deleting redundant nodes or links (pruning). Here the skeletonization algorithm is used. Single nodes of the input layer are deleted based on direct calculation of the influence of the node on the output value for the given data set (Mozer and Smolensky, 1989). The number of selected nodes strongly depends on the parameterization of the skeletonization procedure. However, the ranking of input variables based on a sufficient high number of replicates is much less dependent on the parameterization.

Interpretation of the results of the skeletonization procedure is corroborated by intercorrelations between single variables. Due to substantial autocorrelation, this is especially true for the *temperature* $(d-x)$ and *discharge* $(d-x)$ variables. Comparing the 21:*x*:1, 6:*x*:1 and 3:*x*:1 models (Fig. 4), however, reveals that none of the *temperature* $(d-x)$ and *discharge* $(d-x)$ variables seems to be relevant for the SO_4 dynamics.

5.2. Driving variables

5.2.1. Discharge

Although discharge explains about half of the variance of the SO_4 concentration in the catchment's runoff, the remarkable scatter is a challenge for a more thorough analysis. For example, SO_4 concentration during the highest discharge peaks observed is close to the minimum SO_4 values (Fig. 1). This scatter might be due to the enormous spatial heterogeneity of sulfur pools and residence times in the catchment. On the other hand, part of the scatter might be explained by differing antecedent flow conditions which is emphasized, e.g. by Huntington et al. (1994), Soulsby (1995), and Montgomery and Dietrich (1995).

The suitability of discharge values of preceding days as an indicator for antecedent hydrological conditions obviously is inferior to that of the accumulated runoff sum. Although this indicator has been introduced in an ad hoc manner, it is justified not only by the performance of the model. As discussed below, the relevancy of this indicator is consistent with the understanding of the runoff generation process in the catchment.

5.2.2. Temperature

Corresponding to the SO_4 model presented in this

study, a neural network has been successfully applied to NO_3 time series in the catchment's runoff based on air temperature and discharge (Lischeid et al., 1998b). This confirms the suitability of air temperature as a surrogate for biological activity.

However, air temperature proved not to be a driving variable for SO_4 dynamics by this analysis. This does not imply that biological turnover does not occur as indicated, e.g. by ^{34}S data (Alewell and Gehre, 1999). However, this pool can be considered as a transient store due to steady state demobilization and mineralisation (Houle and Carignan, 1995; Mayer et al., 1995).

On the other hand, air temperature might serve as a surrogate for seasonality. Klemm and Lange (1999) report on a clear seasonal pattern for atmospheric SO_2 mixing ratios measured in the catchment. However, its effect on stream water SO_4 concentration seems to be negligible. This might be due to long residence time. Based on ^{18}O data mean residence time of the catchment's runoff is estimated to be about 3.6 years (Zahn, 1995).

5.2.3. Snowmelt

The impact of snowmelt dynamics on SO_4 is well known. During the onset of snowmelt often very high SO_4 concentrations are observed in meltwater and streamwater (Johannessen and Henriksen, 1978; Helliwell et al., 1998). Thus, the intention was to include this process into the analysis. Unfortunately, snow cover data of the catchment are very rare. The snowmelt indicator used here is based on the approach used by Ostendorf and Manderscheid (1997) to simulate the runoff of the catchment. They determined by inverse modeling a threshold temperature value of $+1°C$ (daily mean value) for the onset of snowmelt. However, including the snowmelt indicator did not improve the performance of the model. As the network error is not systematically higher during snowmelt periods (Fig. 5), it can be concluded that even the snowmelt process itself does not have a significant impact on SO_4 dynamics in the runoff.

5.2.4. Throughfall

Model results indicate that SO_4 concentration in the catchment's runoff is related to that in the throughfall in the long-term at least. It cannot be excluded that short-term effects of throughfall SO_4 concentration (in the range of hours to days) might have an additional effect on solute concentration in the runoff. However, its contribution presumably is rather small, as the model presented here already yields an efficiency of 0.75.

5.3. Interpretation of the dependencies revealed by the model

5.3.1. Functional trend analysis

Due to decreasing sulfate emissions, freshwater sulfate concentration decreased substantially at many North American and European sites in the last two decades (Stoddard et al., 1999). Whereas the time constant of SO_4 sorption in the soil is about some minutes, acidification reversal acts on a time scale of decades due to extended SO_4 stores in the soil (Mörth and Torssander, 1995). The higher the SO_4 store, the less recovery is likely to be seen. In the case of the Lehstenbach catchment, mean depth of the regolith is approximately 30–40 m. The total sulfur store of the regolith is estimated to exceed the annual output by a factor of 70 at least (Manderscheid et al., 2000). This explains why no linear trend is detectable in the catchment's runoff so far.

Obviously, the interplay between different flowpaths that predominate stormflow and baseflow, respectively, explains much of the SO_4 dynamics. This has been confirmed for numerous headwater catchments by chemical hydrograph analysis (Seip et al., 1995; Caissie et al., 1996; Anderson et al., 1997). However, chemical hydrograph separation usually focuses on single short periods, assuming hydrochemical constancy for at least one of the mixing components. Indeed, the identification of simple end members within soils and groundwater has been shown to be highly questionable due to within catchment heterogeneity (Neal et al., 1997). Instead, the neural network approach allows for more flexibility. If some of the driving variables exhibit a clear trend, it provides a tool to investigate the response of the system on a statistical base. This type of a 'functional trend analysis' might be superior to simple trend analysis when the response of the system is restricted to a certain sub-region of the observed phase space.

5.3.2. Stormflow generation processes

Facing the quick response of discharge and runoff chemistry to rainfall, macropore flow (Hornberger et al., 1991; Leaney et al., 1993) or direct infiltration into the streams and bogs might contribute substantially to the runoff generation process. However, in the first years of the study SO_4 concentration in the catchment's runoff significantly exceeds mean concentration (volume weighted) of the throughfall in high flow periods (Fig. 5) and is in the range of soil solution data of about 0.2–0.6 $mmol_c\ l^{-1}$ in the topsoil (Lischeid et al., 1998a). It is concluded that stormflow stream water represents soil solution chemistry of the contributing area rather than precipitation chemistry. This is corroborated by the observation that stormflow runoff usually is predominated by pre-event water (Goodrich and Woolisher, 1991; Anderson et al., 1997).

5.3.3. First storms at the end of the vegetation period

The most dramatic change in the system's response to decreasing sulfur deposition is seen during the first storms at the end of the vegetation period. Soil hydrological and hydrochemical data give strong evidence that these discharge peaks are generated by saturation of the riparian zone close to the streams. With increasing rewetting of the catchment, that is increasing accumulated runoff, an increasing portion of the riparian zone becomes saturated during storms. However, the riparian zone close to the stream is that with the least residence time, and soil solution here adapts most quickly to changing emissions.

Several authors report on flushing effects, washing out SO_4 that accumulated in precedent dry periods (Rice and Bricker, 1995; Evans and Davies, 1998). One reason discussed in the literature is re-oxidation of sulfur when the groundwater level decreases, which is leached when the water level rises again (Dillon and LaZerte, 1992; Caissie et al., 1996). In the Lehstenbach catchment, however, groundwater oxygen data indicate that sulfate reduction is restricted to a limited number of sites in the catchment.

Instead, soil solution becomes more or less immobile in the unsaturated topsoil layer during dry periods. Due to plant root water uptake, SO_4 concentration increases. The first storms after extended dry periods flush out this water. Thus, streamwater quality during these first storms can be used as an early warning indicator for the changing soil chemical status.

The model does not allow explicitly for extrapolation beyond the space of the data offered to the model. However, analysis of the processes that produce the pattern revealed by the model suggests that when recovery of the topsoil layers continues, the first storms at the end of the vegetation period will even exhibit less SO_4 concentration than subsequent storms. This has already been observed in some low order streams in the catchment in the last two years. On the other hand, in two out of six wells installed in 1987 groundwater exhibits a slight, but highly significant steady increase of SO_4 concentration. It cannot be excluded that streamwater recovery observed during storms is compensated for in the long-term by a further increase during baseflow conditions.

6. Conclusions

The results of the study presented here demonstrate the potential of artificial neural networks to analyze hydrochemical time series. They allow for investigating the driving forces of the SO_4 dynamics in a small catchment's runoff and its response to long-term changes of one of the driving forces.

In the catchment studied, a recovery of streamwater due to decreasing sulfate emissions is clearly visible only in a certain sub-region of the phase space. The changing soil chemical status is most clearly reflected during the first discharge peaks at the end of the vegetation period. The conceptual model developed based on these results is consistent with additional data from a comprehensive monitoring measurement program. It is recommended to focus on these events in order to assess beginning long-term changes of a catchment's geochemical status.

Efficient empirical data analysis techniques like artificial neural networks are recommended for the analysis of long-term time series. It is felt that assessing the catchment's future hydrochemical development focusing on these data might be a strategy superior to conventional trend analysis.

Acknowledgements

Thanks to Klaus Moritz, Jochen Bittersohl, Helmut Sager and Heinz Schiller from the Bavarian State Office for Water Management who provided a

substantial part of the data used for the analysis. The remaining data are due to Andreas Kolb, Uwe Hell and the BITÖK laboratory crew. The help of Holger Lange and Eva Plötscher in installing the SNNS code is appreciated. Discussions with Holger Lange and Michael Hauhs gave many helpful hints. The quality of the paper has been improved considerably thanks to Thomas Clair and Colin Neal. Last not least, thanks to Marcel Schaap whose enthusiasm about artificial neural networks encouraged the author. This work was financed by the German Ministry of Education, Research and Technology (BMBF) under grant No. PT BEO 51-0339476B.

References

Alewell, C., Gehre, M., 1999. Patterns of stable S isotopes in a forested catchment as indicators for biological S turnover. Biogeochemistry 47, 319–333.

Anderson, S.P., Dietrich, W.E., Torres, R., Montgomery, D.R., Loague, K., 1997. Concentration–discharge relationships in runoff from a steep, unchanneled catchment. Water Resour. Res. 33, 211–225.

Baum, E.B., Haussler, D., 1989. What size net gives valid generalization?. Neural Comput. 1, 151–160.

Beven, K., 1993. Prophecy, reality and uncertainty in distributed hydrological modelling. Adv. Water Resour. 16, 41–51.

Caissie, D., Pollock, T.L., Cunjak, R.A., 1996. Variation in stream water chemistry and hydrograph separation in a small drainage basin. J. Hydrol. 178, 137–157.

Christophersen, N., Neal, C., 1990. Linking hydrological, geochemical, and soil chemical processes on the catchment scale: an interplay between modeling and field work. Water Resour. Res. 26, 3077–3086.

Clair, T.A., Ehrman, J.M., 1998. Using neural networks to assess the influence of changing seasonal climates in modifying discharge, dissolved organic carbon, and nitrogen export in eastern Canadian rivers. Water Resour. Res. 34, 447–455.

Dillon, P.J., LaZerte, B.D., 1992. Response of the Plastic Lake catchment, Ontario, to reduced sulphur deposition. Environ. Pollut. 77, 211–217.

Evans, C.D., Davies, T.D., 1998. Causes of concentration/discharge hysteresis and its potential as a tool for analysis of episode hydrochemistry. Water Resour. Res. 34, 129–137.

Goodrich, D.C., Woolisher, D.A., 1991. Catchment hydrology. Rev. Geophys. (Suppl.), 202–209.

Hauhs, M., Neal, C., Hooper, R., Christophersen, N., 1996. Summary of a workshop on ecosystem modeling: the end of an era?. Sci. Total Environ. 183, 1–5.

Helliwell, R.C., Soulsby, C., Ferrier, R.C., Jenkins, A., Harriman, R., 1998. Influence of snow on the hydrology and hydrochemistry of the Allt a'Mharcaidh, Cairngorm mountains, Scotland. Sci. Total Environ. 217, 59–70.

Hornberger, G., Germann, P.F., Beven, K.J., 1991. Throughfall and solute transport in an isolated sloping soil block in a forested catchment. J. Hydrol. 124, 81–99.

Hornik, K., Stinchcombe, M., White, H., 1989. Multilayer feedforward networks are universal approximators. Neural Netw. 2, 359–366.

Houle, D., Carignan, R., 1995. Role of SO_4 adsorption and desorption in the long-term S budget of a coniferous catchment on the Canadian Shield. Biogeochemistry 28, 161–182.

Huntington, T.G., Hooper, R.P., Aulenbach, B.T., 1994. Hydrologic processes controlling sulfate mobility in a small watershed. Water Resour. Res. 30, 283–295.

Johannessen, M., Henriksen, A., 1978. Chemistry of snow meltwater: changes in concentration during melting. Water Resour. Res. 14, 615–619.

Kirchner, J.W., Feng, X., Neal, C., 2000. Fractal stream chemistry and its implications for contaminant transport in catchments. Nature 403, 524–527.

Klemm, O., Lange, H., 1999. Trends of air pollution in the Fichtelgebirge Mountains, Bavaria. Environ. Sci. Pollut. Res. 6 (4), 193–199.

Leaney, F.W., Smettem, K.R.J., Chittleborough, D.J., 1993. Estimating the contribution of preferential flow to subsurface runoff from a hillslope using deuterium and chloride. J. Hydrol. 147, 83–103.

Lischeid, G., Alewell, C., Bittersohl, J., Göttlein, A., Jungnickel, C., Lange, H., Manderscheid, B., Moritz, K., Ostendorf, B., Sager, H., 1998a. Investigating soil and groundwater quality at different scales in a forested catchment: the Waldstein case study. Nutr. Cycl. Agroecosyt. 50, 109–118.

Lischeid, G., Lange, H., Hauhs, M., 1998. Neural network modelling of NO_3^- time series from small headwater catchments. Proceedings of the HeadWater'98 Conference held at Meran/Merano, Italy, April 1998, IAHS Publ. no. 248, pp. 467–473.

Luk, K.C., Ball, J.E., Sharma, A., 2000. A study of optimal model lag and spatial inputs to artificial neural network for rainfall forecasting. J. Hydrol. 227, 56–65.

Maier, H.R., Dandy, G.C., 1996. The use of artificial neural networks for the prediction of water quality parameters. Water Resour. Res. 32, 1013–1022.

Manderscheid, B., Schweisser, T., Lischeid, G., Alewell, C., Matzner, E., 2000. Sulfate pools in the weathered bedrock of a forested catchment. Soil Sci. Soc. Am. J. 64, 1078–1082.

Mayer, B., Feger, K.H., Giesemann, A., Jäger, H.-J., 1995. Interpretation of sulfur cycling in two catchments in the Black Forest (Germany) using stable sulfur and oxygen isotope data. Biogeochemistry 30, 31–58.

Montgomery, D.R., Dietrich, W.E., 1995. Hydrologic processes in a low-gradient source area. Water Resour. Res. 31, 1–10.

Mörth, C.-M., Torssander, P., 1995. Sulfur and oxygen isotope ratios in sulfate during an acidification reversal study at Lake Gårdsjön, western Sweden. Water Air Soil Pollut. 79, 261–278.

Mozer, M.C., Smolensky, P., 1989. Skeletonization: a technique for trimming the fat from a network via relevance assessment. Adv. Neural Netw. Inform. Process. Syst. 1, 107–115.

Nash, J.E., Sutcliffe, J.V., 1970. River flow forecasting through

conceptual models, 1. A discussion of principles. J. Hydrol. 10, 282–290.

Neal, C., 1997. A view of water quality from the Plynlimon watershed. Hydrol. Earth Syst. Sci. 1, 743–753.

Neal, C., Hill, T., Hill, S., Reynolds, B., 1997. Acid neutralization capacity measurements in surface and ground waters in the Upper River Severn, Plynlimon: from hydrograph splitting to water flow pathways. Hydrol. Earth Syst. Sci. 3, 687–696.

Oreskes, N., Shrader-Frechette, K., Belitz, K., 1994. Verification, validation, and confirmation of numerical models in the earth sciences. Science 263, 641–646.

Ostendorf, B., Manderscheid, B., 1997. Seasonal modelling of catchment water balance: a two-level cascading modification of topmodel to increase the realism of spatio-temporal processes. Hydrol. Process. 11, 1231–1242.

Peters, H.P., 1991. A Critique for Ecology. Cambridge University Press, Cambridge.

Rice, K.C., Bricker, O.P., 1995. Seasonal cycles of dissolved constituents in streamwater in two forested catchments in the mid-Atlantic region of the eastern USA. J. Hydrol. 170, 137–158.

Riedmiller, M., Braun, H., 1993. A direct adaptive method for faster Backpropagation learning: The Rprop algorithm. Proceedings of the IEEE International Conference on Neural Networks (ICNN), San Francisco, pp. 586–591.

Rumelhart, D.E., McClelland, J.L., 1986. Parallel distributed processing: explorations in the microstructure of cognition, vol. 1. Foundations. MIT Press, Cambridge, MA.

Sager, H., Bittersohl, J., Haarhoff, T., Haberger, I., Moritz, K., 1990. Fate of atmospheric deposition in small catchments depending on local factors. Hydrology in mountainous regions. I — hydrological measurements; the water cycle. Proceedings of two Lausanne Symposia, August 1990. IAHS Publ., 193, pp. 733–740.

Shamseldin, A.Y., 1998. Application of a neural network technique to rainfall-runoff modelling. J. Hydrol. 199, 272–294.

Seip, H.M., Christophersen, N., Mulder, J., Taugbol, G., 1995. Integrating field work and modelling — the Birkenes case. In: Trudgill, S.T. (Ed.). Solute Modelling in Catchment Systems. Wiley, New York, pp. 387–415.

Soulsby, C., 1995. Contrasts in storm event hydrochemistry in an acidic afforested catchment in upland Wales. J. Hydrol. 170, 159–179.

Stoddard, J.L., Jeffries, D.S., Lükewille, A., Clair, T.A., Dillon, P.J., Driscoll, C.D., Forsius, M., Johannessen, M., Kahl, J.S., 1999. Regional trends in aquatic recovery from acidification in North America and Europe. Nature 401, 575–578.

Zahn, M.T., 1995. Transport von Säurebildnern im Untergrund und Bedeutung für die Grundwasserversauerung. Informationsberichte des Bayerischen Landesamtes für Wasserwirtschaft, Heft 3/95, pp. 143–151 (in German).

Zell, A., Mamier, G., Vogt, M., Mache, N., Hübner, R., Döring, S., Herrmann, K.-U., Soyez, T., Schmalzl, M., Sommer, T., Hatzigeorgiou, A., Posselt, D., Schreiner, T., Kett, B., Clemente, G., Wieland, J., Reczko, M., Riedmiller, M., Seemann, M., Ritt, M., DeCoster, J., Biedermann, J., Danz, J., Wehrfritz, C., Werner, R., Berthold, M., Orsier, B., 1995. Stuttgart Neural Network Simulator user manual, Version 4.1. University of Stuttgart, Institute for Parallel and Distributed High Performance Systems, Report No. 6/95.